

Discussion of Results

As a result of dynamic analysis, a good agreement between the results of the theoretical analysis and the computer simulation exists, as shown in Fig. 2. The adequacy of the investigation outlined for preliminary design purposes attests to the system synthesis.

The double integral case³ shown in Fig. 1 was investigated on a similar basis. Since the gyro noise generally is not white, Truncate, Koenigsberg, and Harris⁴ measured the noise power spectrum for different kinds of existing gyros. Expressing the measured data in appropriate theoretical form and calculating the pointing error as a function of bandwidth, a compromise can be made to select the gyro required for a given star tracker. With reference to the results shown, the solutions are presented only to indicate the general characteristics, i.e., mainly the pointing error for a fixed stability criterion. A control system design for a given sensor would most likely have different characteristics because of other systems' nonlinearities. However, for preliminary design purposes, a general statement pertaining to the LST⁵ fine pointing error may be made for general-purpose system synthesis, and the relations describing the governing equations can be modified to other kinds of orbiting spacecraft.

References

- ¹ Harris, R. A., "An Attitude Control System Proposed for the Large Space Telescope Observatory," Feb. 1972, Charles Stark Draper Lab., Cambridge, Mass.
- ² James, H. M., Nichols, N. B., and Phillips, R. S., *Theory of Servo-mechanisms*, MIT Radiation Lab. Series, MIT Press, Cambridge, Mass., 1945.
- ³ Sandhu, G. S., "Rigid Body Mode Pointing Accuracy and Stability Criteria for Large Space Telescope (LST)," TR ASD-PD-1661, Oct. 1972, Teledyne Brown Engineering, Huntsville, Ala.
- ⁴ Truncate, A., Koenigsberg, W., and Harris, R., "Spectral Density Measurements of Gyro Noise," Rept. E-2641, Feb. 1972, Charles Stark Draper Lab., Cambridge, Mass.
- ⁵ "Large Space Telescope, Phase A Final Report," TMX-64726, Dec. 15, 1972, NASA.

Time-Optimal Pitch Control of Satellites Using Solar Radiation Pressure

K. C. PANDE,* M. S. DAVIES,† AND V. J. MODI‡
The University of British Columbia, Vancouver, Canada

Nomenclature

A_i	= control plate area, $i = 1, 2$
C, C_i	= solar parameter, $i = 1, 2$
C^*	= $[2/3(3)^{1/2}]C - [3K_i \sin \psi_e \cos \psi_e]$
I_x, I_y, I_z	= principal moments of inertia of the satellite
K_i	= inertia parameter, $(I_z - I_y)/I_x$
P	= pericenter
Q_ψ	= generalized force due to solar radiation pressure
R_p	= distance between the pericenter and the center of force
i	= inclination of the orbital plane with the ecliptic
n	= $(3K_i \cos 2\psi_e)^{1/2}$, $-\pi/4 < \psi_e < \pi/4$
\bar{u}	= unit vector in the direction of the sun
$u(\theta)$	= control vector
p_0	= solar radiation pressure
x, y, z	= principal body coordinates
x', y', z'	= inertial coordinates

Received December 19, 1973. The investigation was supported by the National Research Council of Canada, under Grant A-2181.

Index category: Spacecraft Attitude Dynamics and Control.

* Graduate Research Fellow, Department of Mechanical Engineering. Student Member AIAA.

† Associate Professor, Department of Electrical Engineering.

‡ Professor, Department of Mechanical Engineering. Member AIAA.

§ Primes indicate differentiation with respect to the orbital angle θ .

x_0, y_0, z_0	= rotating coordinate system with x_0 normal to the orbital plane and y_0 along the local vertical
δ_i	= plate rotation, $i = 1, 2$
e_i	= distance between the center of pressure of control plate and satellite center of mass, $i = 1, 2$
θ	= orbital angle
θ_s, θ_f	= switching time and final time, respectively
μ	= gravitational constant
ζ	= $\omega + \theta + \psi - \tan^{-1}(\tan \phi \cos i)$
ρ, τ	= reflectivity and transmissibility of plate surfaces, respectively
ϕ	= solar aspect angle
ψ, ψ_e	= pitch attitude and its nominal orientation, respectively
ω	= angle between the line of apsides and the line of nodes

Introduction

THE use of solar radiation pressure for attitude stabilization of satellites has been a subject of considerable discussion.¹⁻⁴ Its ability to provide libration damping and general three-axis attitude control to gravity-oriented as well as spinning vehicles has been clearly established.^{5,6} An experiment aboard Mariner IV spacecraft, where solar pressure was used in conjunction with active gyros, demonstrated the effectiveness of the controller in practice.⁷ The feasibility of the concept being well established, the next logical step would be to direct efforts at improving the performance of the system through the implementation of optimal control laws. As the energy required to operate the solar control plates is quite small and could be generated easily through the use of solar cells, the performance index need only include the damping time which is of prime concern.

Time-optimal control of multidegree-of-freedom systems, such as the coupled roll-yaw-pitch motions of a satellite, generally involves software complexity as the solution of a two-point boundary-value problem is required. On the other hand, a single-degree-of-freedom system may lend itself to an analytical synthesis of the time-optimal switching criterion. This is significant since if successful, it not only could be applied to several situations of practical importance (platform pitch control of a spinning satellite, e.g., the proposed magnetic-solar hybrid control system⁸ or pure pitch control of a gravity gradient system as in the case of COSMOS-149⁹) but may also suggest switching

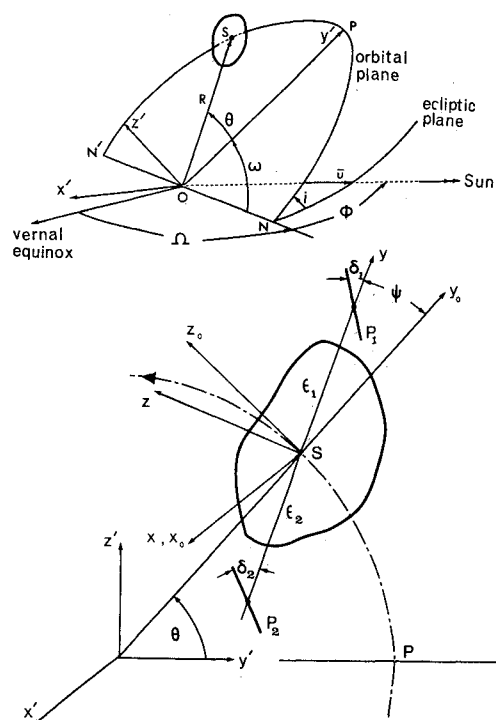


Fig. 1 Geometry of motion.

laws that are likely to be efficient in controlling the general motion.

This Note investigates the problem of controlling the pitch attitude of satellites in minimum time. The optimal control law is synthesized which leads to an important relationship between disturbances, control plate areas and moment arms, and the corresponding minimum damping times.

Formulation of the Problem

Figure 1 shows an unsymmetrical satellite executing planar pitch libration ψ , with the center of mass S moving in a circular orbit about the center of force O . The governing equation of motion is well known

$$\psi'' + 3K_i \sin \psi \cos \psi = Q_\psi \quad (1)$$

The solar pressure controller consists of two highly reflective plates P_1 and P_2 which are permitted rotations δ_1 and δ_2 , respectively, in the orbital plane. The center of pressure of each plate is taken to lie on the satellite y axis (could be anywhere on the yz -plane) so as to yield a pure pitch moment. The moment generated by the controller is⁶

$$Q_\psi = \pm C_i |\sin(\delta_i + \zeta)| \sin(\delta_i + \zeta) \cos \delta_i, \quad i = 1, 2 \quad (2)$$

(+ for P_1 , - for P_2)

where the solar parameter is defined as

$$C_i = (2\rho p_0 R_p^3 / \mu I_x) A_i e_i (1 - \sin^2 \phi \sin^2 i) \quad (3)$$

Through a judicious choice of the plate to be operated (P_1 or P_2), in accordance with the angle $(\delta_i + \zeta)$, Q_ψ may be controlled in sign. The magnitude of the control moment, $|Q_\psi|$, varies with both the angle ζ and the control variable δ_i . Its maximum with respect to δ_i occurs at

$$\delta_{im} = \tan^{-1} \left[-\frac{3}{2} \tan \zeta \pm \left\{ \frac{9}{4} \tan^2 \zeta + 2 \right\}^{1/2} \right] \quad (4)$$

where the \pm signs apply for $\tan \zeta \geq 0$, respectively. The variation of $|Q_\psi|_{\max}$ with ζ is shown in Fig. 2a where $C_1 = C_2 = C$ is assumed for convenience. The system is thus able to provide a value $|Q_\psi|_{\max} = [2/3(3)^{1/2}]C$ at all times. The governing equation of motion (1) may now be presented as

$$\psi'' + 3K_i \sin \psi \cos \psi = u(\theta) \quad (5)$$

with

$$- [2/3(3)^{1/2}]C - 3K_i \sin \psi_e \cos \psi_e \leq u(\theta) \leq [2/3(3)^{1/2}]C - 3K_i \sin \psi_e \cos \psi_e$$

A symmetrical band on the control

$$|u(\theta)| \leq C^* = [2/3(3)^{1/2}]C - |3K_i \sin \psi_e \cos \psi_e| \quad (6)$$

is considered here for convenience. Its effect is only to yield a slightly conservative bound on the control either on the plus or the minus side depending on the nominal attitude ψ_e .

Time-Optimal Synthesis

Using the state variables $x_1 = \psi$, $x_2 = \psi'$ and linearizing about the nominal attitude $\psi = \psi_e$, the system (5) can be expressed in the form

$$\dot{\mathbf{x}}' = \mathbf{Ax} + \mathbf{Bu} \quad (7)$$

where

$$\mathbf{x} = \begin{bmatrix} x_1 \\ x_2 \end{bmatrix}, \quad \mathbf{A} = \begin{bmatrix} 0 & 1 \\ -n^2 & 0 \end{bmatrix}, \quad \mathbf{B} = \begin{bmatrix} 0 \\ 1 \end{bmatrix} \quad \text{and} \quad |u(\theta)| \leq C^*$$

An admissible control $\mathbf{u}(\theta)$, transferring the system state from $\mathbf{x}(0)$ to $\mathbf{x}(\theta_f) = \mathbf{0}$, is easily found to be governed by

$$\int_0^{\theta_f} \Phi(-\tau) \mathbf{B} \mathbf{u}(\tau) d\tau = -\mathbf{x}(0) \quad (8)$$

where $\Phi(\theta)$ denotes the state-transition matrix with $\theta_0 = 0$.

The solution for $\mathbf{u}(\theta)$ bringing the system state to rest in minimum θ_f is well known to be $\mathbf{u}(\theta) = \pm C^*$, with the number of switches depending upon the initial state of the system.¹⁰

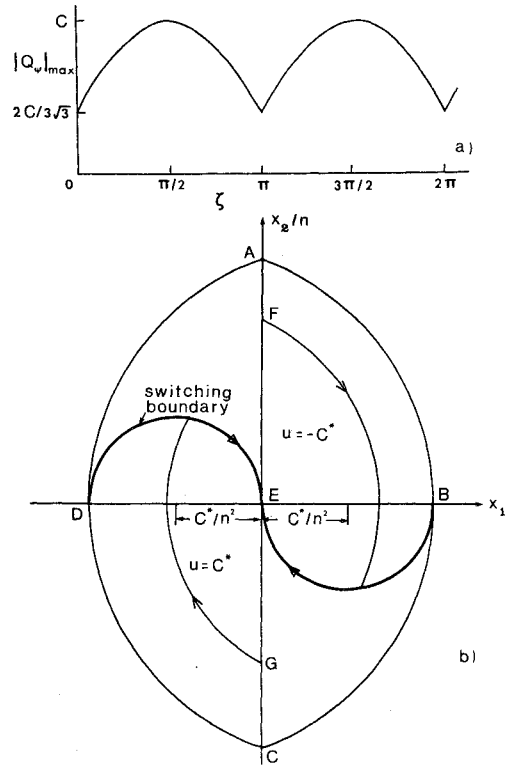


Fig. 2 a) Variation of $|Q_\psi|_{\max}$ with ζ . b) Phase plane portrait of the system.

Considering initial states that can be driven to rest in a single switch, the control takes the form

$$u(\theta) = K_1, \quad 0 \leq \theta < \theta_s \\ u(\theta) = K_2, \quad \theta_s \leq \theta \leq \theta_f \quad (9)$$

where $|K_1| = |K_2| = C^*$.

Substitution in Eq. (8) leads to

$$K_1 = n \{ -nx_1(0)(\sin n\theta_f - \sin n\theta_s) + x_2(0)(\cos n\theta_f - \cos n\theta_s) \} / \Delta \quad (10a)$$

$$K_2 = n \{ nx_1(0) \sin n\theta_s + x_2(0)(1 - \cos n\theta_s) \} / \Delta \quad (10b)$$

where

$$\Delta = \sin(n\theta_f - n\theta_s) - \sin n\theta_f + \sin n\theta_s \quad (10c)$$

The proper signs of K_1 and K_2 are best obtained from the phase plane portrait of the optimally controlled system (Fig. 2b). The trajectories are circular arcs with centers at $x_1 = \pm C^*/n^2$, $x_2 = 0$ for $u = \pm C^*$, respectively. The switching boundary is composed of semicircles passing through the origin. For any initial state $\mathbf{x}(0)$, the system state moves on the switching boundary for $\theta_s \leq \theta \leq \theta_f$ as shown in the figure. It is apparent that all initial conditions lying within the region ABCDA of the phase diagram can be driven to the origin with a single switch of the control. For optimal response, the control $u(\theta)$ assumes the value $u = -C^*$ if the system state lies above the switching boundary and $u = +C^*$ if it is below the switching boundary.

Equations (10) may now be solved to obtain the switching time θ_s and the final time θ_f for a given initial condition. This yields the open-loop realization of the control in the form $u = u(\theta)$. On the other hand, use of the switching boundary yields the feedback realization $u = u(\mathbf{x})$, which makes the system self-correcting to slight deviations of the state vector.

Of particular interest are impulsive disturbances which a satellite is likely to encounter such as micrometeorite impacts. The phase portrait immediately yields the maximum impulsive disturbance from which the satellite can be brought to rest in a single switch of the control and the error amplitude during the process as

$$|\tilde{x}_2(0)|_{\max} = 2(2)^{1/2} \quad (11a)$$

$$|\tilde{x}_1(\theta)|_{\max} = \{1 + \tilde{x}_2^2(0)\}^{1/2} - 1 \quad (11b)$$

where the normalized state variables \tilde{x}_1 and \tilde{x}_2 are defined as

$$\tilde{x}_1(\theta) = n^2 x_1(\theta)/C^* \quad (11c)$$

$$\tilde{x}_2(\theta) = n x_2(\theta)/C^* \quad (11d)$$

The variation of the normalized error amplitude with the initial impulsive disturbance is shown in Fig. 3a. The switching and the final times obtained by solving Eqs. (10) are also presented as functions of the impulsive disturbance (Fig. 3b).

System Response and Results

In order to ascertain the applicability of the optimal control law synthesized from linear theory to the actual nonlinear system, the response of both the linearized and nonlinear equations governing the motion was evaluated. The two systems were subjected to the same disturbance and control.

Figures 4a and 4b show response plots indicating the effect of the inertia parameter to be negligible for the pitch attitude nominally along the local vertical. As anticipated, the open-loop and the feedback response of the linear system are identical. On the other hand, the open-loop control system is unable to bring the nonlinear system to rest exactly. The feedback system accomplishes this, however, the nonlinear system state approaching the origin asymptotically using a number of switches of the control. In order to avoid any relay chatter, it appears advisable to use only a single switch for the actual nonlinear system as well and employ a passive device to damp the small residual motion in the neighborhood of the origin.

Figures 4c and 4d present the response of a satellite stabilized in an arbitrary pitch attitude. Note that the gravity torque now represents a destabilizing effect which the controller must neutralize in addition to countering the disturbance. The longer damping time required with a higher value of the inertia parameter clearly reflects a greater reduction in the value of C^* for increased K_i .

It appears interesting to estimate the performance of the controller when applied to an actual satellite. Considering the proposed Canadian Communications Technology Satellite (CTS)

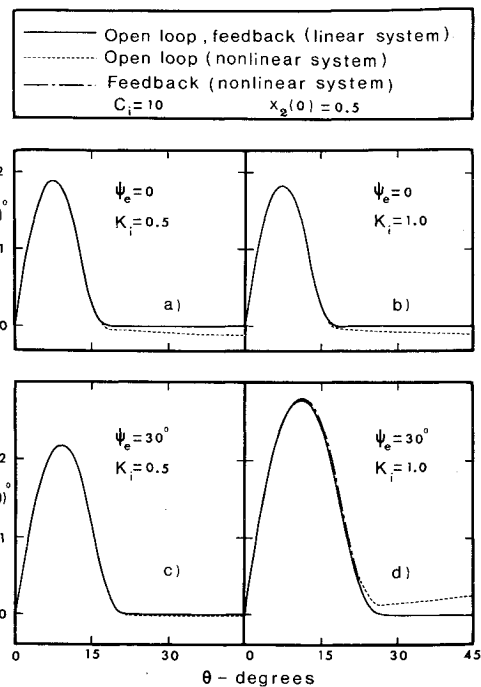


Fig. 4 System response to impulsive disturbance.

at synchronous altitude, the value of $C_i \approx 10$ results with $A_i = 2.5$ ft² and $\epsilon_i = 10$ ft. When subjected to an extremely severe impulsive disturbance $x_2(0) = 0.5$, damping times of the order of 20° of the orbit are attained (Fig. 4) which appear promising.

It may be pointed out that the constraint $|Q_\psi| \leq [2/3(3)^{1/2}]C$ represents the most adverse situation, as $|Q_\psi|$ may attain a value as large as C during certain orbital positions (Fig. 2a). The performance of the controller, therefore, would always exceed the responses presented here (Fig. 4). Furthermore, the control system does not require any mass expulsion schemes or active gyros. Its semipassive character thus promises an increased satellite lifespan.

References

- 1 Sohn, R. L., "Attitude Stabilization by Means of Solar Radiation Pressure," *ARS Journal*, Vol. 29, 1959, pp. 371-373.
- 2 Hilbard, R. R., "Attitude Stabilization Using Focused Radiation Pressure," *ARS Journal*, Vol. 31, 1961, pp. 844-845.
- 3 Crocker, M. C. II, "Attitude Control of a Sun-Pointing Spinning Spacecraft by Means of Solar Radiation Pressure," *Journal of Spacecraft and Rockets*, Vol. 7, No. 3, March 1970, pp. 357-359.
- 4 Modi, V. J. and Flanagan, R. C., "Librational Damping of a Gravity Oriented System using Solar Radiation Pressure," *Aeronautical Journal, Royal Aeronautical Society*, Vol. 75, Aug. 1971, pp. 560-564.
- 5 Modi, V. J. and Kumar, K., "Coupled Librational Dynamics and Attitude Control of Satellites in Presence of Solar Radiation Pressure," *Astronautical Research 1971, Proceedings of the XXII Congress of the International Astronautical Federation*, L. G. Napolitano, editor-in-chief, D. Reidel Publishing Co., Dordrecht, The Netherlands, 1973, pp. 37-52.
- 6 Modi, V. J. and Pande, K. C., "Solar Pressure Control of a Dual-Spin Satellite," *Journal of Spacecraft and Rockets*, Vol. 10, No. 6, June 1973, pp. 355-361.
- 7 Scull, J. R., "Mariner IV Revisited, or the Tale of the Ancient Mariner," presented at the 20th Congress of the International Astronautical Federation, Argentina, Oct. 1969.
- 8 Modi, V. J. and Pande, K. C., "Magnetic-Solar Hybrid Attitude Control of Dual-Spin Spacecraft," *Journal of Spacecraft and Rockets*, to be published.
- 9 Sarychev, V. A., "Aerodynamic Stabilization System of the Satellites," *Proceedings of the International Colloquium on Attitude Changes and Stabilization of Satellite*, Paris, Oct. 1968, pp. 177-179.
- 10 Pontryagin, L. S., Boltyanskii, V. G., Gamkrelidze, R. V., and Mischenko, E. F., *The Mathematical Theory of Optimal Processes*, Pergamon, New York, 1964, pp. 26-34.

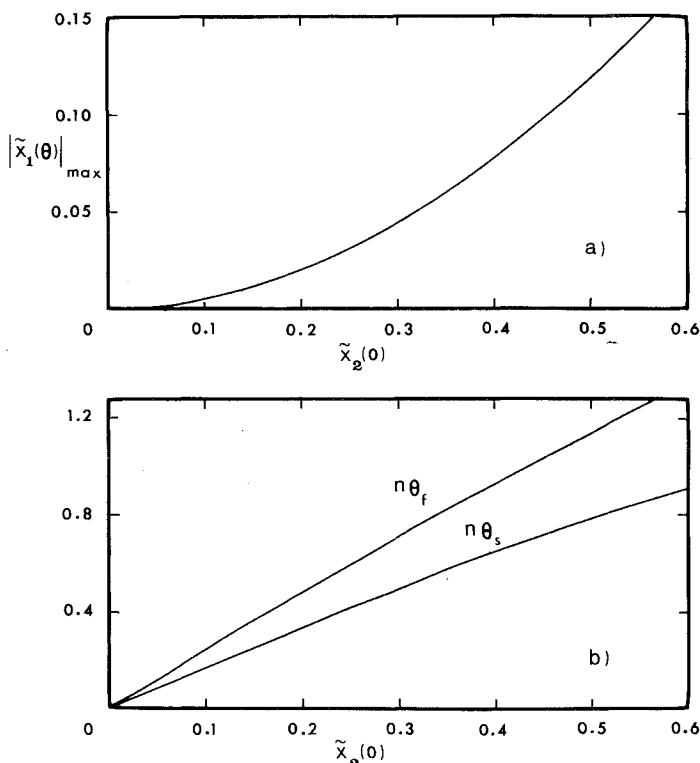


Fig. 3 a) Variation of transient amplitude $|\tilde{x}_1(\theta)|_{\max}$ with initial condition $\tilde{x}_2(0)$. b) Variation of switching time θ_s and final time θ_f with initial condition $\tilde{x}_2(0)$.